

Science 7, November 1997

Vol. 278. no. 5340, pp. 1104 - 1106, DOI: 10.1126/science.278.5340.1104

Observed Hemispheric Asymmetry in Global Sea Ice Changes

D. J. Cavalieri, P. Gloersen, C. L. Parkinson, J. C. Comiso, H. J. Zwally

Abstract

From November 1978 through December 1996, the areal extent of sea ice decreased by 2.9 ± 0.4 percent per decade in the Arctic and increased by 1.3 ± 0.2 percent per decade in the Antarctic. The observed hemispheric asymmetry in these trends is consistent with a modeled response to a carbon dioxide-induced climate warming. The interannual variations, which are 2.3 percent of the annual mean in the Arctic, with a predominant period of about 5 years, and 3.4 percent of the annual mean in the Antarctic, with a predominant period of about 3 years, are uncorrelated.



Observed Hemispheric Asymmetry in Global Sea Ice Changes

D. J. Cavalieri; P. Gloersen; C. L. Parkinson; J. C. Comiso; H. J. Zwally

Science, New Series, Vol. 278, No. 5340 (Nov. 7, 1997), 1104-1106.

Stable URL:

<http://links.jstor.org/sici?sici=0036-8075%2819971107%293%3A278%3A5340%3C1104%3AOHAIGS%3E2.0.CO%3B2-1>

Science is currently published by American Association for the Advancement of Science.

Your use of the JSTOR archive indicates your acceptance of JSTOR's Terms and Conditions of Use, available at <http://www.jstor.org/about/terms.html>. JSTOR's Terms and Conditions of Use provides, in part, that unless you have obtained prior permission, you may not download an entire issue of a journal or multiple copies of articles, and you may use content in the JSTOR archive only for your personal, non-commercial use.

Please contact the publisher regarding any further use of this work. Publisher contact information may be obtained at <http://www.jstor.org/journals/aaas.html>.

Each copy of any part of a JSTOR transmission must contain the same copyright notice that appears on the screen or printed page of such transmission.

JSTOR is an independent not-for-profit organization dedicated to creating and preserving a digital archive of scholarly journals. For more information regarding JSTOR, please contact support@jstor.org.

Observed Hemispheric Asymmetry in Global Sea Ice Changes

D. J. Cavalieri,* P. Gloersen, C. L. Parkinson, J. C. Comiso, H. J. Zwally

From November 1978 through December 1996, the areal extent of sea ice decreased by 2.9 ± 0.4 percent per decade in the Arctic and increased by 1.3 ± 0.2 percent per decade in the Antarctic. The observed hemispheric asymmetry in these trends is consistent with a modeled response to a carbon dioxide-induced climate warming. The interannual variations, which are 2.3 percent of the annual mean in the Arctic, with a predominant period of about 5 years, and 3.4 percent of the annual mean in the Antarctic, with a predominant period of about 3 years, are uncorrelated.

Model experiments simulating future conditions assuming a gradual increase in atmospheric CO_2 show various hemispheric asymmetries (1–4); in particular, some suggest that Arctic sea ice will decrease, whereas Antarctic sea ice will decrease substantially less than Arctic sea ice (3) or may even increase (4). Here we report observational evidence of a hemispheric asymmetry in global sea ice changes from late 1978 through 1996.

Analyses of passive microwave satellite observations (5, 6) have suggested that the extent of the Arctic sea ice cover (the total area with ice concentration greater than 15%) shrank at 2.5% per decade from 1978 to 1987, whereas there were only insignificant changes in the Antarctic sea ice cover. A more recent study (7) that extended the analysis to 1994 found that Arctic ice extent continued to decrease and that the Antarctic ice also was decreasing by $0.7 \pm 0.6\%$ per decade.

We have extended the passive microwave satellite observations through December 1996, using data from the Nimbus 7 Scanning Multichannel Microwave Radiometer (SMMR) (8) and three Defense Meteorological Satellite Program (DMSP) Special Sensor Microwave Imager (SSM/I) (9) sensors. The SMMR was launched in October 1978 and was fully operational until August 1987; data were collected every other day through most of that period. The first of the three SSM/Is was launched on the DMSP F8 spacecraft in June 1987, the second was launched on the F11 spacecraft in November 1991, and the third was launched on the F13 spacecraft in March 1995. A period of almost 6 weeks of data overlap in 1987 provides a means of cross-calibrating the SMMR and SSM/I sea ice

data sets. Overlap between the DMSP F8 and F11 spacecraft is only 2 weeks, but the overlap between the F11 and F13 spacecraft is 5 months. Our analyses show that these sensors required intercalibration, because during the overlap periods the residual differences of several percent in sea ice extent and area (the sum of the products of pixel area times ice concentration for ice concentration greater than 15%) would adversely affect the trend analysis (10).

After corrections for residual instrument drift, bad or missing data, and false sea ice signals over ice-free ocean areas (11), comparisons of sea ice concentrations from different sensors (12) during overlap periods still revealed significant differences, particularly in marginal ice zones. Much of the SMMR-SSM/I difference is attributed to the greater sensitivity of SSM/I to atmospheric water vapor (13, 14). The initial uncorrected differences for daily Arctic and Antarctic sea ice extents and areas were 2 to 4% during the overlap periods. To lessen these differences, we developed linear relations between the measured radiances for corresponding channels from each sensor during the overlap periods. These relations were used to adjust the SSM/I algorithm radiance tie points relative to the SMMR tie points. These adjustments reduced the ice extent and area differences to about 1%. Further adjustments of the ice-free ocean tie points

reduced the differences in ice extents and areas to 0.02 and 0.4%, respectively, for the SMMR and SSM/I F8 data, 0.04 and 0.6% for the SSM/I F8 and F11 data, and 0.06 and 0.6% for the SSM/I F11 and F13 data (15).

Accurate determination of long-term sea ice trends depends in large part on accounting for shorter-term fluctuations, the largest of which is the annual cycle of ice growth and decay (Fig. 1). Day-to-day variations, resulting from storms and currents, and annual variations are removed by calculating the monthly deviations (Fig. 2). We used a band-limited regression (BLR) technique (5, 16) to determine the trend in each of the monthly deviation time series shown in Fig. 2 for the period November 1978 through December 1996 (Table 1). This technique suppresses fluctuations having periods less than one-quarter the data record length of 18.2 years, including intra-annual fluctuations not already removed in the process of computing monthly deviations and some interannual fluctuations. The method entails substituting a truncated form of the sinc function matrix for the usual correlation matrix in a weighted least-squares formulation for obtaining a linear fit to the data. The sinc function, described in (5), is a function of the form $(\text{sinc}x)/x$ that is used here as a multiple-window filtering function. This method effectively applies a narrow band-pass filter centered about zero frequency before extracting the trend line.

Superimposed on the monthly deviation time series shown in Fig. 2 are two trend lines for each hemisphere. One corresponds to the BLR result and the other to an ordinary least-squares regression (OLR) fit of the monthly deviation data. The difference in slopes of the Antarctic trend lines is attributed to the BLR filtering of fluctuations with periods shorter than about 4.5 years, including the predominant 3-year fluctuations observed in the curve smoothed with an annual running mean, also shown in Fig. 2B. Thus, the BLR technique may provide a more accurate determination of the long-term trends through its filtering of shorter-term fluctuations. The rate of change per decade for the

Table 1. Trends in Arctic and Antarctic sea ice covers during the period 1978–1996 from a BLR analysis. The OLR results are given in parentheses. For all the BLR results, the confidence level exceeds 99% (29).

Parameter	Slope \pm SD ($10^6 \text{ km}^2 \text{ year}^{-1}$)	Rate of change (% per decade)
Arctic		
Extent	-0.0345 ± 0.0053	-2.9 ± 0.4 (-2.9 ± 0.3)
Area	-0.0294 ± 0.0044	-2.9 ± 0.4 (-2.9 ± 0.4)
Antarctic		
Extent	$+0.0143 \pm 0.0026$	$+1.3 \pm 0.2$ ($+1.0 \pm 0.5$)
Area	$+0.0138 \pm 0.0025$	$+1.6 \pm 0.3$ ($+1.3 \pm 0.6$)

Laboratory for Hydrospheric Processes, NASA Goddard Space Flight Center, Code 971, Greenbelt, MD 20771, USA.

*To whom correspondence should be addressed.

Arctic ice extents is $-2.9 \pm 0.4\%$, whereas the rate for the Antarctic is $+1.3 \pm 0.2\%$ (Table 1). The fluctuations of sea ice extent observed in the monthly deviation time series in each hemisphere (Fig. 2, A and B) are uncorrelated ($r = -0.06$), but there is a small negative correlation ($r = -0.44$) for the smoothed time series. In contrast to the Arctic, the Antarctic ice extents showed no significant trend from 1978 through 1993. From late 1993 through 1996, the Antarctic ice extent remained above the 18-year mean.

Our study and earlier studies indicate that, overall, the Arctic sea ice cover has been decreasing, although not monotonically, during the past 20 years. Nimbus 5 electrically scanning microwave radiometer (ESMR) data show that Arctic ice extent increased from 1973 through 1976, before the decrease from 1979 through 1986 revealed in the SMMR data (17). For our entire time series (see Fig. 1A), the four lowest summertime extents occurred during the last 7 years, with the two lowest extents occurring in 1990 and 1995. The 1990 minimum has been attributed to a combination

of high springtime temperatures and an anomalous high-latitude circulation pattern that year (18) and may be related to a recent decrease of sea level pressure in the central Arctic (19). Also, variations in Arctic sea ice extent and its overall trend correspond both spatially and temporally to variations in surface air temperatures over the past three decades (20).

Although we lack overlap between the ESMR and SMMR data that would permit precise matching of these two data sets, it appears that the maximum Antarctic sea ice extent since 1972 occurred in 1973. Analysis using ESMR data, combined with NOAA-Navy analyses based in part on passive microwave data, showed that Antarctic

sea ice decreased during the mid-1970s (21) and increased in the late 1970s and early 1980s (22). The increase in Antarctic sea ice during the SMMR and SSIM period (Fig. 2B), although occurring in spite of a warming trend in the Southern Hemisphere (23), conforms with recent results on changes in the length of the sea ice season in the Southern Ocean from 1988 through 1994. The length of the sea ice season decreased in some areas while increasing in others, but overall the area of increases exceeded the area of decreases by about 20% (24).

Although model simulations do not incorporate all the complexities in the climate system, they can provide valuable insights

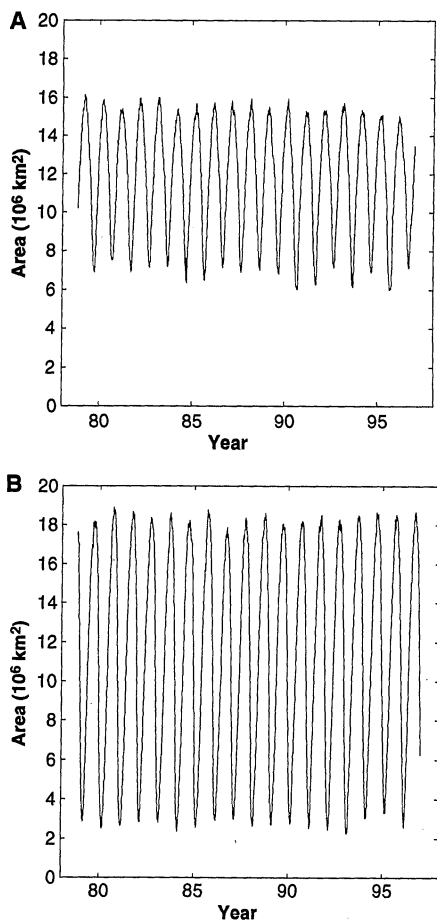


Fig. 1. Sea ice extents derived from multisensor single-day records for (A) the Arctic and (B) the Antarctic.

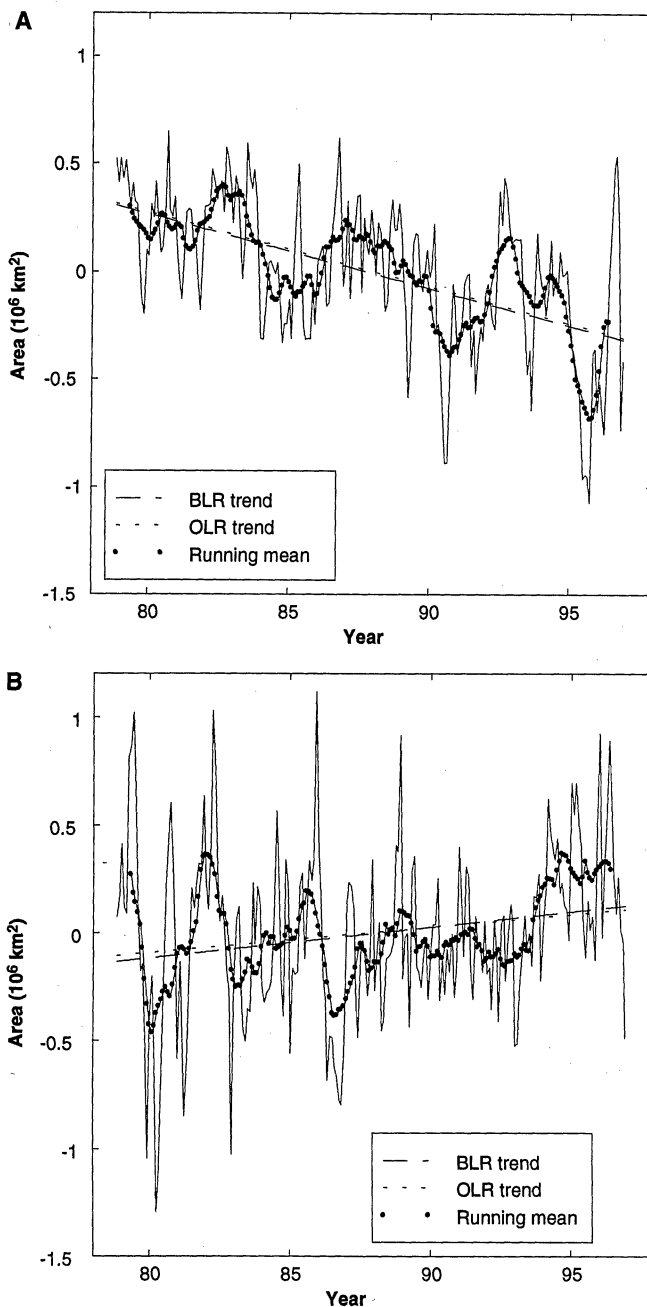


Fig. 2. Monthly deviations in sea ice extent (light solid curve) with both BLR (long-dashed) and OLR (short-dashed) trend lines for (A) the Arctic and (B) the Antarctic. A 12-month running mean (curve with dots) is also shown for both.

and comparative results. The increase in Antarctic sea ice and decrease in Arctic sea ice reported here are consistent with results from a General Circulation Model (GCM) study in which CO₂ levels were increased gradually (4). Other GCM simulations, though, show slight decreases in Antarctic sea ice extent and thickness (3). GCM simulations of CO₂-induced climate change patterns generally agree on some large-scale features such as the amplification of wintertime warming at high northern latitudes but disagree particularly at high southern latitudes (25). This study also indicates a surface air cooling over the Atlantic sector of the Southern Ocean in austral summer (the season when we observe a maximum positive trend in the ice extents). In these GCM experiments, the hemispheric difference in the climate response results in part from the influence of the thermal inertia of the much larger ocean area in the Southern Hemisphere. Sea ice growth in the Southern Ocean, along with slight lowering of the surface water temperature, are attributed to a general freshening of southern circumpolar surface water and the resultant reduction of convective mixing (3, 4). The continuing sea ice data record shows significant interannual and decadal variability that helps provide the basis for developing a better understanding of the various processes driving the observed changes.

REFERENCES AND NOTES

1. R. J. Stouffer, S. Manabe, K. Bryan, *Nature* **342**, 660 (1989).
2. J. M. Murphy and J. F. B. Mitchell, *J. Clim.* **8**, 57 (1995).
3. H. B. Gordon and S. P. O'Farrell, *Mon. Weather Rev.* **125**, 875 (1997).
4. S. Manabe, M. J. Spelman, R. J. Stouffer, *J. Clim.* **5**, 105 (1992).
5. P. Gloersen and W. J. Campbell, *Nature* **352**, 33 (1991).
6. O. M. Johannessen, M. W. Miles, E. Bjørge, *ibid.* **376**, 126 (1995).
7. E. Bjørge, O. M. Johannessen, M. W. Miles, *Geophys. Res. Lett.* **24**, 413 (1997).
8. P. Gloersen and F. T. Barath, *IEEE J. Oceanic Eng. OE-2*, 172 (1977).
9. J. P. Hollinger, *DMSP Special Sensor Microwave/Imager Calibration/Validation, Final Report Vol. 1* (Naval Research Laboratory, Washington, DC, 1989).
10. Correction for ice extent and area differences from the various sensors during the overlap periods was critical to obtaining unbiased long-term trends. In Bjørge *et al.* (7), a correction for SMMR-SSM/I differences was mentioned but none for SSM/I F8-F11 differences. Bjørge *et al.* used a two-step procedure to match ice concentrations for the SMMR-SSM/I correction. Our matching of algorithm coefficients was somewhat comparable to their procedure, but then we additionally matched ice extents and areas during the overlap periods.
11. Each data set was subjected to careful quality control, including the identification and subsequent correction or removal of bad data. Residual instrumental drift in the SMMR radiances used in the sea ice algorithm was reduced, by means of a procedure used previously (26), to values well below the instrument noise levels (8). The SSM/I drifts similarly determined were found to be below or at the instrument

- noise values (9) for the SSM/I radiances used in the sea ice algorithm (19 GHz horizontally and vertically polarized, 22 GHz vertically polarized, and 37 GHz vertically polarized) and so were ignored. Data gaps were filled by performing spatial and temporal interpolations. Additional corrections made to the SMMR and SSM/I single-day sea ice concentration grids included the removal of false sea ice signals in the vicinity of the shoreline and over ice-free ocean areas. These were accomplished through the application of a coastline correction algorithm operating on the three image pixels nearest the coast, and also of monthly climatological sea surface temperature thresholds.
12. The calculation of Arctic and Antarctic sea ice concentrations needed to compute sea ice extents and sea ice areas utilizes methods used previously for the SMMR (26) and SSM/I (27) data sets. The details of generating a consistent set of sea ice extents and areas from the SMMR and SSM/I sensors are discussed elsewhere (28). Since the publication of this report (28), DMSP F13 SSM/I data through 31 December 1996 were added, but we followed the same procedure in preparing the data for analysis.
13. D. J. Cavalieri, K. M. St. Germain, C. T. Swift, *J. Glaciol.* **41**, 455 (1995).
14. Other differences giving rise to different ice concentrations include differences in sensor altitudes and view angles; differences in weather filter thresholds and algorithm tie points; and different overpass times, tidal phases, and diurnal effects.
15. The upper limit of the ice extent and area errors for both the Arctic and Antarctic is obtained by calculating the standard deviations of the ice extent and area differences from the F11 and F13 SSM/I during their 5-month overlap period. The estimates are all about 0.3% of the annual mean value. It is noteworthy that the equatorial crossing times of the two spacecraft differ by 45 min, so that even this estimate includes real fluctuations of the ice covers. Of central importance in this study is not absolute accuracy but the consistency of measurements throughout the data record.
16. C. Kuo, C. R. Lindberg, D. J. Thomson, *Nature* **343**,

- 709 (1990).
17. C. L. Parkinson and D. J. Cavalieri, *J. Geophys. Res.* **94**, 14499 (1989).
18. M. C. Serreze, J. A. Maslanik, J. R. Key, R. F. Kokaly, D. A. Robinson, *Geophys. Res. Lett.* **22**, 2183 (1995).
19. J. E. Walsh, W. L. Chapman, T. L. Shy, *J. Clim.* **9**, 480 (1996).
20. W. L. Chapman and J. E. Walsh, *Bull. Am. Meteorol. Soc.* **74**, 33 (1993).
21. G. Kukla and J. Gavin, *Science* **214**, 497 (1981).
22. H. J. Zwally, C. L. Parkinson, J. C. Comiso, *ibid.* **220**, 1005 (1983).
23. T. H. Jacka and W. F. Budd, in *International Conference on the Role of the Polar Regions in Global Change*, G. Weller, C. L. Wilson, B. A. B. Severin, Eds. (Geophysical Institute and Center for Global Change and Arctic System Research, University of Alaska, Fairbanks, AK, 1991), pp. 63–70.
24. C. L. Parkinson, *Antarct. Res. Ser.*, in press.
25. J. Raisanen, *Clim. Dynam.* **13**, 197 (1997).
26. P. Gloersen *et al.*, *Arctic and Antarctic Sea Ice, 1978–1987: Satellite Passive Microwave Observations and Analysis* (NASA, SP-511, Washington, DC, 1992).
27. D. J. Cavalieri *et al.*, *J. Geophys. Res.* **96**, 21989 (1991).
28. D. J. Cavalieri, C. L. Parkinson, P. Gloersen, H. J. Zwally, *NASA Technical Memorandum 104647* (1997).
29. The confidence level was determined with a Student's *t* test in which the number of degrees of freedom is obtained by subtracting the number of calculated parameters from the number of windows used in the multiple window filtering.
30. The SSM/I data sets were provided by the National Snow and Ice Data Center in Boulder, CO. We thank S. Fiegles, M. Martino, and J. Saleh for their efforts in reprocessing and correcting the SMMR and SSM/I data sets and J. A. Maslanik and J. Stroeve for their help in checking the final sea ice concentrations. This work was supported by NASA's polar program.

15 August 1997; accepted 2 October 1997

Abiotic Selenium Redox Transformations in the Presence of Fe(II,III) Oxides

S. C. B. Myneni,* T. K. Tokunaga, G. E. Brown Jr.

Many suboxic sediments and soils contain an Fe(II,III) oxide called green rust. Spectroscopic evidence showed that selenium reduces from an oxidation state of +VI to 0 in the presence of green rust at rates comparable with those found in sediments. Selenium speciation was different in solid and aqueous phases. These redox reactions represent an abiotic pathway for selenium cycling in natural environments, which has previously been considered to be mediated principally by microorganisms. Similar green rust-mediated abiotic redox reactions are likely to be involved in the mobility of several other trace elements and contaminants in the environment.

The redox chemistry of polyvalent elements determines their solubility, bioavailability, and toxicity in geologic environments (1, 2). This is apparent in the case of Se, which occurs in the environment in +VI, +IV, 0, and -II oxidation states and in several organic forms (2–4). Their concentration and biogeochemical transformations determine the activity of Se in the environment. Although Se is essential to animal life at low concentrations and its deficiency is known to cause white muscle

disease in sheep, Se compounds at high concentrations are carcinogenic and teratogenic (4). The higher valent Se forms are more soluble, and their reduction in soil to the less reactive Se(0) form has generally been considered to be facilitated primarily by soil organic acids (5) and microorganisms (6, 7). However, many suboxic geologic environments contain green rust (GR), which is a mixed Fe(II), Fe(III) oxide, and it has been shown to catalyze redox reactions (8–10). Here we show how GR medi-